

ZT Scan DIA with deconvolution improves the MS/MS purity, coverage, and identification rate in metabolomics analysis compared to DDA and SWATH

Triston Groff¹, Yunwon Kang², Matt Ward¹, Paul RS Baker², Jason Causon³, and Gary J. Patt¹

¹Washington University in St. Louis, USA; ²Sciex, USA; ³Sciex, Canada

This technical note demonstrates the suitability of ZT Scan DIA acquisition on the SCIEX ZenoTOF 8600 system, coupled with MS-DIAL processing, for untargeted metabolomics. With ZT Scan DIA, comprehensive MS2 coverage of MS1 features is achieved, and the resulting deconvoluted spectra are less chimeric than those from either DDA or SWATH, leading to higher putative MS/MS identification rates.

Data-independent acquisition (DIA) has seen limited adoption in metabolomics due to persistent concerns about highly chimeric MS/MS spectra, which impair compound identification. Even with narrow isolation windows, conventional data-dependent acquisition (DDA) workflows often yield co-isolated fragment ions, reducing spectral purity. Established deconvolution approaches, including retention-time-based (RTDec) and database-assisted (DBDec) methods, offer partial mitigation but remain constrained by co-elution complexity, chromatographic variability, and incomplete spectral library coverage, particularly for structurally diverse small molecules.

Here, quadrupole-axis deconvolution (Q1Dec), implemented via ZT Scan DIA acquisition on the ZenoTOF 8600 system, is evaluated as an

alternative strategy for untargeted metabolomics. ZT Scan DIA employs a rapidly scanning, sliding isolation window combined with Zeno trapping to reconstruct high-quality, DDA-like MS/MS spectra independent of isolation width [1-3]. Using a *Leptospiriosis* infection model in human vascular endothelial cells, ZT Scan DIA was benchmarked against Top N DDA and variable-window SWATH. Results demonstrate improved spectral clarity, increased identification rates, and enhanced MS/MS coverage, highlighting ZT Scan DIA as a robust solution for reducing chimeric interference and advancing DIA-based metabolomics workflows (Figure 1).

Key features of ZT Scan DIA data Q1 deconvolution

- **Quadrupole-axis deconvolution (Q1Dec) with ZT Scan DIA** enables precursor-specific fragment assignment by using a sliding isolation window across the Q1 dimension, resulting in cleaner, less chimeric MS/MS spectra.
- **Comprehensive MS/MS coverage (>99% of features)** is achieved through DIA acquisition that fragments all detectable precursors, which ensures consistent detection of both high- and low-abundance metabolites.
- **Multiplexed deconvolution (Q1Dec + RTDec) in MS-DIAL** combines orthogonal strategies to resolve both co-isolated and co-eluting species.

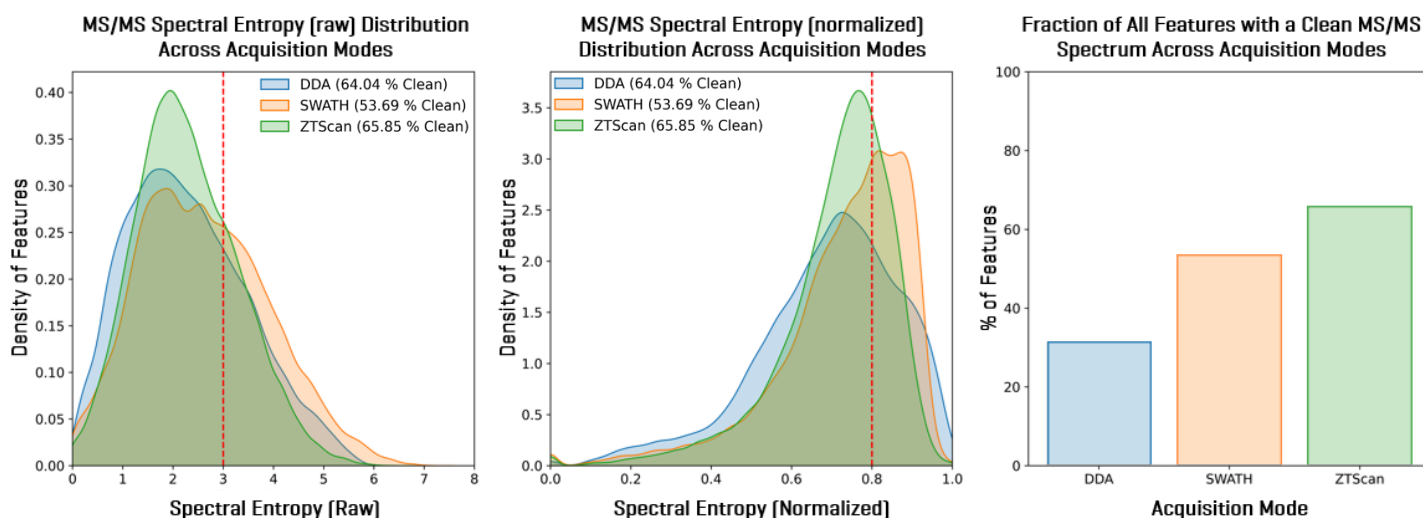


Figure 1. [Left] Raw spectral entropy distributions of features, [Center] normalized spectral entropy distributions of features, and [Right] the percentages of the total features with a clean MS/MS spectrum across all the samples for the three data-acquisition modes [ZT Scan DIA 2.0, SWATH, and DDA] obtained from the deconvoluted PeakID data exported from the "All-Modes" MS-DIAL project. Lower entropies are cleaner than higher entropies. For the Left and Right panels, the dashed red line at 3.0 and 0.8, respectively, show the threshold for classification as either "clean" or "noisy."

Introduction

Similarly to the early days of proteomics, DIA workflows (which often employ wide isolation windows to comprehensively fragment all precursors) have not yet gained widespread traction in metabolomics due to concerns of highly chimeric spectra, and data-dependent analysis (DDA, also known as IDA) workflows with narrow isolation windows (≤ 1 Da) are still preferred. This is because chimeric spectra, arising from the co-isolation and fragmentation of additional precursor ions alongside the targeted precursor of interest, are particularly concerning in metabolomics, given the vast chemical space of small molecules compared with peptides, which exhibit predictable fragmentation patterns. The contamination of a query MS/MS spectrum with additional fragment ions from unwanted precursors hinders identification via spectral similarity scoring against experimentally obtained reference spectra of pure standards.

Even narrow, unit-resolved DDA isolation windows often produce chimeric spectra. Moreover, the common practice of selecting the top N precursors per cycle with dynamic exclusion in untargeted DDA experiments precludes conventional retention-time deconvolution (RTDec), because no MS² elution profile is acquired [4-6]. RTDec resolves co-eluting interferences by correlating the chromatographic elution profiles [apex, width, and peak shape] of precursor and product ions, as routinely performed in GC-MS, SWATH, AIF, or targeted DDA analyses. However, RTDec has its shortcomings and often fails to correctly correlate common class-specific diagnostic fragment ions produced by many similar analytes to a single precursor ion [7]. Furthermore, wide and asymmetric chromatographic peaks, those common in HILIC-based metabolomics experiments, pose additional challenges for precursor and product ion chromatogram correlation.

Database-assisted deconvolution (DBDec) offers an acquisition-independent alternative by reconstructing chimeric query spectra through linear combinations of library reference spectra [8-12]. Yet, especially for metabolomics, DBDec remains limited by incomplete library coverage and has not been optimized with wide isolation windows, reducing its effectiveness for novel compounds and wide-window DIA schemes such as SWATH.

First conceptualized over a decade ago [13], quadrupole-axis deconvolution (Q1Dec) has only recently become practically viable for DIA metabolomics [14]. Building on early hardware implementations [15], the new ZenoTOF 8600 system's ZT Scan DIA mode acquires spectra by rapidly scanning a sliding isolation window across the mass range in fine steps while leveraging Zeno trapping to enhance duty cycle and sensitivity. These data can be deconvoluted to yield a Q1 precursor ion selection window as narrow as 0.9 Da. Q1Dec overcomes the hardware limitation of isolating a narrow precursor region because its ability to eliminate unwanted precursors stems from the sliding window's step size, rather than its width. It is also compatible with all the previously mentioned deconvolution strategies, enabling the multiplexed application of RTDec, Q1Dec, and DBDec within modern

software such as MS-DIAL and DecoID, yielding cleaner spectra and higher library identification rates than either conventional DDA or SWATH.

In this technical note, we evaluate the suitability of three acquisition modes available on the ZenoTOF 8600 (DDA, SWATH, and ZT Scan DIA) for untargeted metabolomics in human vascular endothelial cells infected with *Leptospirosis* from three different bacterial strains. Using MS-DIAL for data processing and a variety of spectral databases for identification, we show that ZT Scan DIA outperforms Top 85 DDA and 80 variable-width SWATH methods in terms of putative MS/MS identification rate, MS/MS coverage (in the case of DDA), and MS/MS spectral quality after deconvolution. Through simulations using the exported MS-DIAL data, we also show that approximately 50% of the DDA features with MS/MS spectra are chimeric, and that, after deconvolution, ZT Scan DIA data produces cleaner MS/MS spectra than either method.

Materials and methods

Sample preparation: HMEC-1 cells were plated in 60 mm dishes at a density of 800,000 cells/dish in MCDB 131 medium supplemented with 10% fetal bovine serum, 10 ng/mL epidermal growth factor, 1 μ g/mL hydrocortisone, and 10 mM glutamine as per recommendations from the American Tissue Culture Collection (ATCC) and allowed to attach overnight. The following day, the medium was changed and inoculated with either PBS [UI], *Leptospira biflexa serovar Patoc* strain Patoc-1 [LbP], *Leptospira interrogans serovar Copenhageni* strain Fiocruz L1-130 [LiC], or *Leptospira interrogans serovar Manilae* strain L495 [LiM] at a multiplicity of infection of 20. After 24 h, the medium was removed, the cell layer was washed twice with warm 0.85% saline, and a 2:2:1 acetonitrile:methanol:water extraction solvent was applied. The dish was incubated for 5 minutes on dry ice, then the cell layer was scraped off into 1.5 mL microcentrifuge tubes, vortexed for 30 sec, flash-frozen in liquid nitrogen for 1 min, and stored on dry ice until sample isolations were complete. Afterward, all samples were sonicated for 5 min and subjected to two rounds of vortexing for 30s, flash-freezing in liquid nitrogen for 1 min, and sonication for 5 min. Samples were stored at -20°C overnight to precipitate proteins. The following day, samples were centrifuged at 18,000 RCF at 4°C for 10 min, and the supernatant was removed and dried with a SpeedVac Concentrator. Meanwhile, the protein pellet was resuspended in 400 μ L 100 mM NaOH and dissolved with four cycles of vortexing for 10 s and heating at 95°C for 5 min. Protein concentration was measured with a BCA assay, and the dried metabolite pellets were resuspended in a 2:1 acetonitrile: water solution at 1 μ L/2.5 μ g protein in each sample. The suspension was then subjected to two cycles of 5 min sonication and 1 min vortexing and then incubated at 4°C overnight. The following day, samples were centrifuged at 18,000 RCF at 4°C for 10 min, and the supernatant was transferred to glass LC-MS vials for analysis on the ZenoTOF 8600 system.

Chromatography: Prepared samples were resolved by HPLC using a HILICON iHILIC-(P) Classic column [100 x 2.1 mm, 5 μ m, 200 Å; P/N 161.122.0520] equipped with a guard column [HILICON iHILIC-(P) Classic Guard, 5 μ m, 200 Å, P/N 161.122.0520]. The column was maintained at 45 °C. Mobile phase A consisted of 5.0% acetonitrile in water containing 20 mM ammonium bicarbonate, 1% ammonium hydroxide, and 5 μ M medronic acid. Mobile phase B was 95% acetonitrile in water with no additives. The gradient conditions are shown in Table 1.

Table 1. Chromatographic elution conditions

Time (min)	Flow rate (mL/min)	% Mobile phase B
0	0.25	90
1	0.25	90
12	0.25	35
12.5	0.25	25
14.5	0.25	25
15	0.25	90
16.5	0.4	90
20	0.4	90
20.5	0.25	90
22	0.25	90

Mass spectrometry: Analysis of the endothelial metabolite extracts was performed on the ZenoTOF 8600 system equipped with an Optiflow Pro ion source and an electrospray ionization (ESI) probe. Instrument calibration was maintained using the automated calibrant

delivery system (CDS), which calibrated every 15 samples with the new universal calibration solution for both ionization modes. Samples were analyzed by collision-induced dissociation (CID) in positive- and negative-ion modes, using 3 different scan modes: DDA, SWATH, or ZT Scan DIA. For this technical note, only positive-ion mode data were used to investigate chimeric spectral deconvolution. Instrument parameter settings are provided in Table 2.

Data processing. All raw data [*.wiff2] were processed in MS-DIAL v5.6 (build 5.6.250820-alpha; hereafter “MS-DIAL 5.6”) by using the parameter set summarized in Table 3. The full processing workflow comprised centroiding, peak detection, adduct annotation, compound identification, and cross-sample alignment. Identification was performed against multiple MS/MS spectral libraries in *.msp format, with parameter settings tuned per library to account for differences in curation level, instrument provenance, and spectral density [Table 3].

For the NIST23 spectral library, an in-house curated *.msp derivative was generated to ensure compatibility with the MS-DIAL scoring framework and to standardize metadata. Specifically, additional compound-level annotations (for example, InChIKey, formula, exact mass) were programmatically populated via the PubChem API, and the library was filtered to retain only entries acquired on high-resolution platforms by using ESI or APCI ionization [16,17]. This step was intended to constrain the search space to spectra most consistent

Table 2. Instrument parameter settings for DDA, SWATH, and ZT Scan DIA on the ZenoTOF 8600 system

Parameter	ZenoTOF 8600 system	
	POS	NEG
Curtain gas (CUR)	40 psi	40 psi
Ion source gas 1 (GS1)	50	50
Ion source gas 2 (GS2)	50	50
CAD gas (CAD)	7	7
Source temperature (TEM)	400	400
Ion spray voltage (IS)	5500 V	-4500 V
QJet declustering potential (DP)	20 V	-20 V
Collision energy (CE) TOFMS	8 V	-8 V
Collision energy (CE) TOFMS/MS	30 V	-30 V
Zeno threshold	2,000,000 cps	2,000,000 cps
TOF and TOFMS/MS start mass	70 Da; 40 Da	70 Da; 40 Da
TOF and TOFMS/MS stop mass	1000 Da	1000 Da
TOFMS accumulation time [Acc]	100 ms	100 ms
Time bins to sum (TOF MS; TOF MS/MS)	4; 6	4; 6
TOFMS/MS accumulation time [Acc]	5 ms	5 ms
Collision energy spread (CES)	0	0
DDA selection	Top 85	Top 85
Exclusion time criteria	6 s after 2 occurrences	6 s after 2 occurrences
Minimum TOF MS intensity	300 cps	300 cps
Number of windows	80	80
Window width	variable	variable
Collision energy spread (CES)	0	0
Calculated accumulation time	6.6 ms	6.6 ms
Scanning Q1 window	7.4 Da	7.4 Da
ZT Scan 2.0 Deconvoluted Q1 resolution	1.48 Da	1.48 Da

Table 3. MS-DIAL 5.6 parameter settings and metabolomics databases used for processing

DataBase	Medicine For Malaria Ventures - Pathogen Box	MoNA - Fiehn HILIC	MoNA - MassBank	MSMS-Public_all-pos-VS19	NIST23 Tandem MS/MS (High resolution only)
Reference URL	https://gnps.ucsd.edu/ProteoSAFe/gnpslibrary.jsp?library=MMV_POSITIVE	https://mona.fiehnlab.ucdavis.edu/downloads	https://mona.fiehnlab.ucdavis.edu/downloads	https://zenodo.org/record/13261737	https://scix.com/products/spectral-library
MassRangeBegin	40	40	40	40	40
MassRangeEnd	1000	1000	1000	1000	1000
RtTolerance	100	100	100	100	100
Ms1Tolerance	0.01	0.01	0.01	0.01	0.01
Ms2Tolerance	0.025	0.025	0.025	0.025	0.025
RelativeAmpCutoff	0.01	0.01	0.01	0.01	0.01
AbsoluteAmpCutoff	0	0	0	0	0
WeightedDotProductCutOff	0.6	0.6	0.6	0.6	0.6
SimpleDotProductCutOff	0.6	0.6	0.6	0.6	0.6
ReverseDotProductCutOff	0.8	0.8	0.8	0.8	0.8
MatchedPeaksPercentageCutOff	0.25	0.25	0.25	0.25	0.25
TotalScoreCutoff	0.8	0.8	0.8	0.8	0.8
MinimumSpectrumMatch	2	2	2	2	2
IsUseTimeForAnnotationFiltering	False	False	False	False	False
IsUseTimeForAnnotationScoring	False	False	False	False	False

with the acquisition conditions used in this study, while minimizing ambiguity introduced by low-resolution or orthogonal ionization data.

For each processing run, MS-DIAL results were exported at two levels. At the per-sample level, PeakID tables and associated experimental MS/MS spectra [*.msp] were retained. At the study level, the AlignmentID table, which represents globally aligned features across all samples, was exported for downstream filtering and summary analysis.

To systematically evaluate the influence of acquisition strategy and deconvolution, data were processed both independently and in combination. Specifically, three single-mode projects were created (DDA-only, SWATH-only, and ZT Scan DIA-only), followed by an "All-Modes" project in which all acquisitions were jointly aligned to generate a consensus feature list. Within the DIA-based projects (SWATH and ZT Scan DIA), additional processing branches were implemented to isolate the effects of spectral deconvolution. Initial

processing was performed with deconvolution disabled ("NoDec") by unchecking both "Run RT deconvolution" and "Run Q1Dec" in the Spectrum Deconvolution settings (Figure 2). The same datasets were then reprocessed with one or more deconvolution strategies enabled.

For SWATH data, two configurations were considered: NoDec and RT-based deconvolution (RTDec). For ZT Scan DIA 2.0, four configurations were evaluated: NoDec, RTDec, quadrupole-axis deconvolution (Q1Dec), and the combined RTQ1Dec condition. PeakID tables and MS/MS spectra were exported after each processing pass, enabling direct comparison of feature-level outcomes across deconvolution strategies. Alignment tables were exported only for the highest deconvolution level applied to each dataset to avoid redundancy.

Before export, alignment results were filtered to retain only confidently characterized features, defined here as those matched to a reference database and exhibiting an MS-CleanR blank ratio <0.05. Beyond this automated filtering, minimal manual curation was performed.

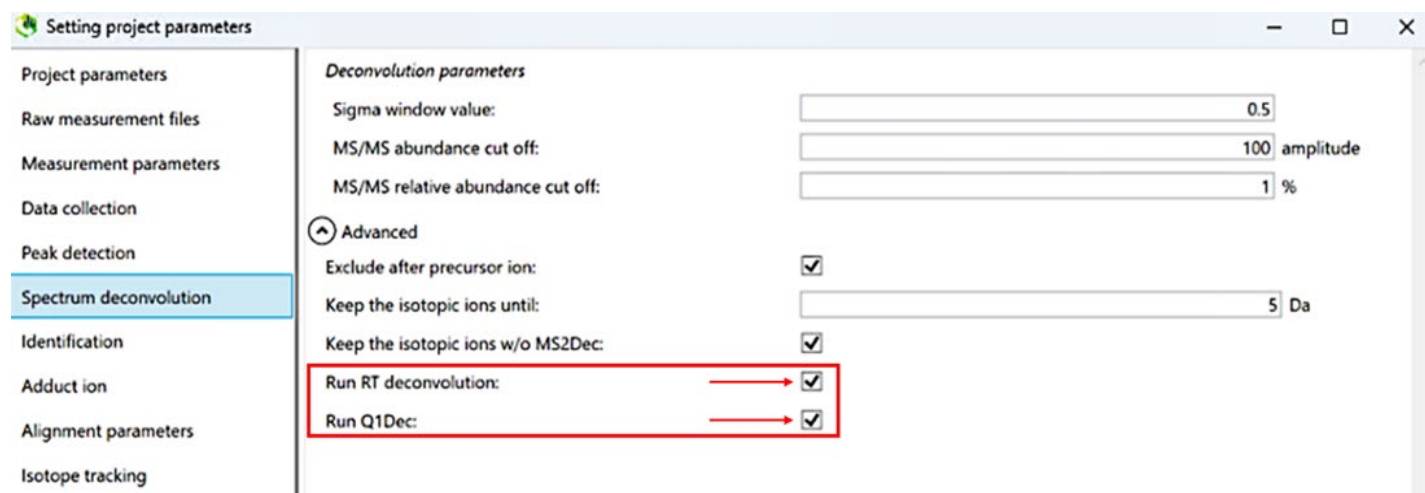


Figure 2. Spectrum deconvolution options in MS-DIAL 5.6. RTDec and Q1Dec are options for deconvolution; both are recommended for the best results when processing ZT Scan DIA data.

Consequently, the dataset retains the expected artifacts of large-scale untargeted processing, including duplicated features due to imperfect alignment, partial peak integration, and occasional suboptimal library matches. While these would typically be addressed in a fully optimized metabolomics workflow, they were considered acceptable within the scope of the present benchmarking and simulation-focused analysis.

Data analysis and *in silico* simulations. All downstream analysis was conducted in Python, with MS-DIAL PeakID tables imported as Pandas DataFrames to enable flexible, feature-level manipulation. Each entry in the PeakID table encodes a discrete chromatographic feature with associated metadata, including retention-time boundaries (left, apex, right), precursor m/z , experimental MS/MS spectrum, peak shape descriptors (Gaussian similarity, ideal slope, symmetry), and annotation details.

Feature counts were derived by summing the row counts across all PeakID tables. From this population, subsets were defined based on data completeness and annotation status. Features with recorded MS/MS spectra were first isolated, and within this subset, library-matched features were identified by using MS-DIAL [annotation tag codes 330 and 430].

To further stratify spectral quality, an entropy-based classification scheme [18,19] was applied following conventions established by the MassBank of North America (MoNA). MS/MS spectra were designated as “clean” when they satisfied dual criteria of raw spectral entropy <3.0 and normalized spectral entropy <0.8, as calculated by using the SpectralEntropy Python package. This step provides an orthogonal quality metric independent of library matching or simulated classification as chimeric or non-chimeric based on PeakID tables and is particularly useful in the context of not only DIA data but also DDA data; spectral chimerism is prevalent in both types of data.

To simulate spectral chimerism and assess the effects of deconvolution, the analysis was restricted to features with observed MS/MS spectra. For each feature A, pairwise comparisons were performed against all other features B within the same sample to evaluate potential co-isolation and resolvability.

Chimerism was defined operationally based on joint m/z and chromatographic overlap criteria. Feature A was classified as chimeric if any feature B exhibited (i) a precursor m/z falling within the isolation window of A and (ii) overlapping chromatographic boundaries (i.e., $B_{\text{left}} < A_{\text{right}}$ and $B_{\text{right}} > A_{\text{left}}$). This definition captures both direct co-elution and partial temporal overlap scenarios relevant to DIA acquisitions (and potentially DDA acquisitions).

Deconvolution performance was modeled by using three complementary frameworks:

- **Database-assisted deconvolution (DBDec)**, applicable across all acquisition modes, evaluates whether co-isolated features can be separated based on MS/MS dissimilarity.

Here, A is considered unresolved from B if the spectral similarity between their experimental MS/MS spectra exceeds 0.8, calculated by using the entropy similarity metric with a 20 ppm tolerance. Notably, the reference “database” in this context is sample-specific and constructed directly from the ensemble of observed spectra in the PeakID table. This captures the challenge of reconstructing a convolved query spectrum as a linear combination of database spectra when the database contains too many candidates with shared peaks.

- **Retention-time deconvolution (RTDec)**, applied to SWATH and ZT Scan DIA 2.0 data, leverages chromatographic orthogonality. Features are considered resolvable when they exhibit sufficient divergence in peak apex ($\Delta RT \geq 5$ s), relative peak width (>20% difference), or peak shape (any descriptor differing by >0.2). This reflects the practical heuristics commonly embedded in deconvolution algorithms.
- **Quadrupole-axis deconvolution (Q1Dec)**, unique to ZT Scan DIA 2.0, exploits differences in precursor isolation. Resolution is achieved when the absolute m/z separation between features exceeds the Q1 step size (0.8 Da), which is consistent with the acquisition stepping scheme.

All possible combinations of these deconvolution strategies (for example, RTDec alone, DBDec alone, RTDec+DBDec, Q1Dec alone, etc.) were evaluated. For each combination, the IDs of features that met the resolution criteria were tracked and stored, enabling detailed post hoc inspection and visualization. A summarized results table, capturing counts and classifications across all scenarios, was exported as a CSV for reporting and downstream interpretation.

Results and discussion

Untargeted metabolomics workflows are fundamentally constrained by the realities of gas- and liquid-phase chemistry in the mass spectrometer, where the idealized assumption that a single precursor yields a single clean product-ion spectrum is rarely met in practice. Instead, particularly under high-throughput acquisition modes and in complex biological matrices, multiple co-eluting or near-isobaric precursors are frequently co-isolated and fragmented simultaneously. The resulting product-ion spectra, commonly referred to as chimeric spectra, represent a convolution of fragment ions derived from multiple molecular species.

From a practical standpoint, chimeric spectra are not the exception; they are an intrinsic feature of data-dependent and, even more so, data-independent acquisition strategies. In dense chromatographic space, precursor isolation windows inevitably capture co-eluting species with overlapping m/z values. This co-isolation leads to multiplexed fragmentation events, producing spectra that no longer map cleanly to a single chemical entity. While such multiplexing can increase acquisition efficiency, it introduces ambiguity in spectral

Table 4. Summary of features, features with associated MS/MS spectra, and % of raw spectra that are chimeric.

Sample ID	# of Features detected			# of Features with MS/MS			% Raw chimeric MS/MS spectra		
	DDA	SWATH	ZT Scan DIA	DDA	SWATH	ZT Scan DIA	DDA	SWATH	ZT Scan DIA
LbP_1	7255	8663	6287	3541	8660	6278	71.3	99.7	99.7
LbP_2	7148	8484	5539	3503	8477	5531	71.5	99.7	99.5
LbP_3	8020	9273	6008	3639	9269	5996	72.8	99.7	99.7
LbP_4	6729	7952	5236	3429	7951	5232	68.2	99.8	99.5
LiC_3	8110	9864	5798	3740	9563	5794	71.9	99.8	99.6
LiM_3	6831	7877	5663	3474	7875	5660	71.2	99.6	99.5
LiM_4	6823	8024	5828	3467	8022	5825	71.0	99.7	99.5
UI_1	7525	8872	5781	3756	8871	5776	72.1	99.8	99.6
UI_3	7463	8411	5477	3724	8409	5473	70.5	99.6	99.5
UI_4	7458	8420	5429	3762	8418	5423	70.1	99.7	99.7
Average	7336	8554	5705	3604	8552	5699	71.0	99.7	99.6

interpretation, which directly affects downstream identification confidence.

The consequences of spectral convolution are multifaceted. First, the presence of fragment ions originating from multiple precursors can obscure or distort the characteristic fragmentation patterns required for confident library matching. Diagnostic ions may be suppressed, shifted in relative intensity, or masked entirely by overlapping fragments from co-isolated species. Second, the inclusion of unrelated fragment ions can artificially inflate spectral similarity scores against incorrect library entries, increasing the likelihood of false-positive identifications. This effect is particularly pronounced in large-scale spectral library searches, where even modest overlap in fragment ion space can yield misleading matches when the underlying spectra are not pure.

Addressing the impact of chimeric spectra is therefore a critical step toward improving confidence in untargeted workflows. Recent advances in acquisition strategies, such as ZT Scan DIA, and in computational deconvolution approaches have begun to mitigate these challenges by either reducing the frequency of precursor co-isolation or disentangling mixed spectra after acquisition. In the following sections, we evaluate how effectively these strategies improve spectral purity and, consequently, the reliability of compound identification in complex metabolomic samples.

DIA-based workflows generate comprehensive MS/MS coverage of the metabolome

The ultra-fast acquisition rate of the ZenoTOF 8600 system, combined with the sensitivity gains of the Zeno trap, enables a 5 ms dwell time for MS/MS spectrum acquisition, allowing 85 precursors per cycle to be acquired in a 1s duty cycle in DDA, which results in ~50% of features in MS-DIAL having an associated MS/MS spectrum. Despite leveraging the improved scan speed, DDA still cannot achieve the MS/MS acquisition rates possible with SWATH or ZT Scan DIA methods – both of which obtained MS/MS spectra for >99% of features [Table 4]. As expected, the SWATH DIA and ZT Scan DIA data generated raw MS/MS spectra that are almost entirely chimeric. However, the DDA data also showed a high level of chimeric interference.

MS/MS spectra acquired with DDA have significant chimeric interference

Simulation using DDA PeakID tables shows that >50% of detected features [A] have at least one co-eluting feature [B] with an m/z value within the precursor isolation window [Table 4], demonstrating that DDA spectra are frequently chimeric, consistent with previous observations [5]. Although DDA is considered the benchmark for generating high-quality MS/MS spectra for database matching, substantial contamination persists due to the finite quadrupole isolation width (~1.0 Da on SCIEX systems). Narrowing this window is the only hardware-based approach to reduce chimericity, but it does not eliminate it and comes at the cost of reduced precursor transmission efficiency.

Compared to DIA, DDA exhibits lower levels of chimeric interference; however, it results in reduced MS/MS coverage and the inability to perform robust MS/MS-level quantitation. This is particularly true for low-abundance features. These limitations arise from the stochastic nature of precursor selection and dynamic exclusion, which also constrain data-driven deconvolution approaches.

Given that MS/MS contamination is largely unavoidable across acquisition strategies, computational deconvolution is required. ZT Scan DIA enables a complementary approach by fragmenting each precursor multiple times as the quadrupole isolation window steps across the m/z space. This produces a characteristic intensity distribution across sequential MS/MS scans, allowing fragment ions to be associated with their precursors along the Q1 dimension. In MS-DIAL, this strategy [Q1Dec] can be combined with retention time-based deconvolution, thereby improving spectral purity and coverage for downstream identification.

Q1Dec: A novel deconvolution approach based on a dynamic quadrupole with ZT Scan DIA acquisition

In ZT Scan DIA acquisition, the quadrupole mass filter moves a precursor ion transmission window across the full precursor m/z range in fine, overlapping steps that are ~1/5 the width of the isolation

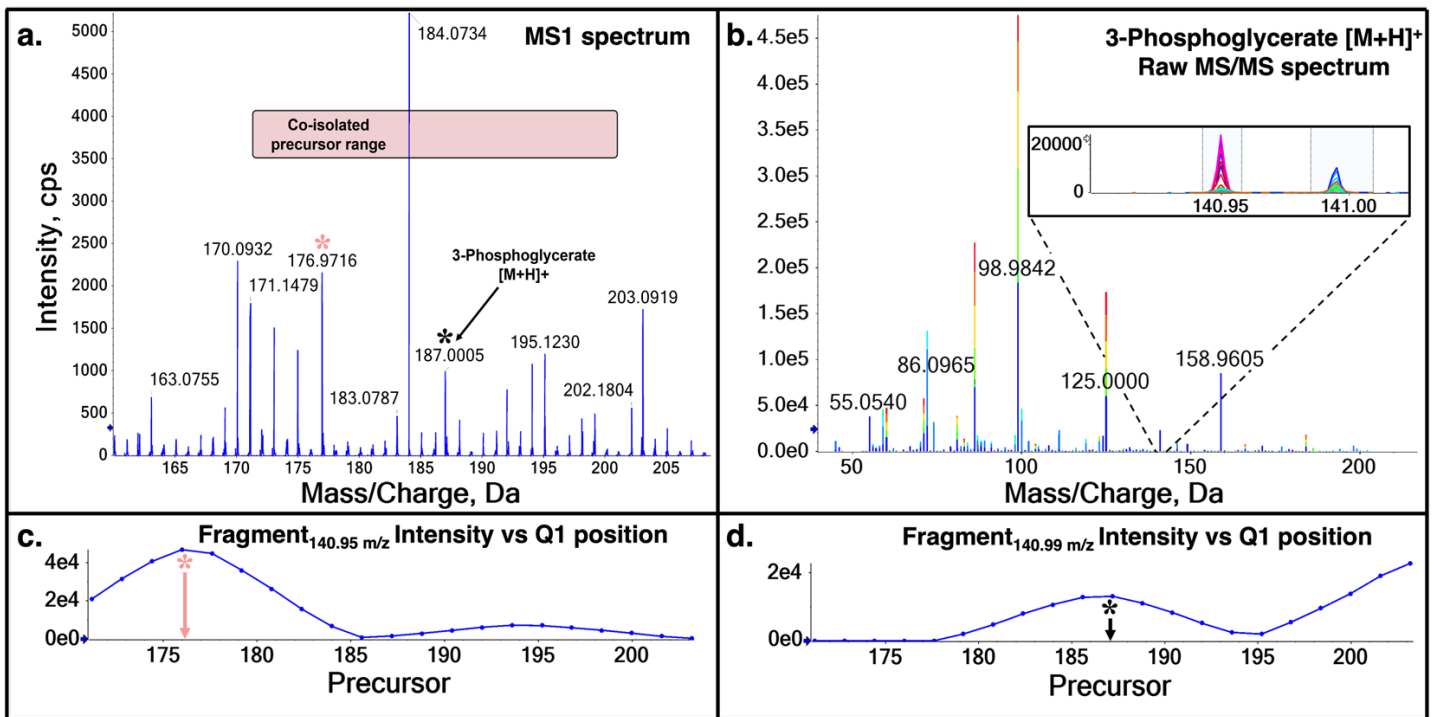


Figure 3. Figure: [a] An MS1 spectrum showing a 3-phosphoglycerate [M+H]⁺ [3-PGA] ion and other co-isolated precursor ions, and [b] the resulting convolved MS/MS spectra, which isolate 3-PGA. Summing the intensities of the [c] 140.95 *m/z* ion and [d] 140.99 *m/z* fragments as Q1 slides points to the precursor they originate from.

window. As the window slides, a given precursor ion gradually enters the transmission window, reaches maximum transmission when centered, and then exits. Consequently, the intensities of its fragment ions are recorded across multiple consecutive MS/MS scans, each corresponding to a slightly different Q1 position [1-2].

When the intensity of a specific fragment ion is plotted against the center position of the isolation window (i.e., along the Q1 axis), it produces a characteristic triangular envelope whose apex corresponds directly to the true precursor *m/z* [Figure 3]. Because of this relationship, fragment ions from co-isolated precursors with different *m/z* values can be assigned to their respective precursors by using a process called quadrupole-axis deconvolution (Q1Dec). Q1Dec exploits these intensity profiles to trace each fragment ion back to its originating precursor, even when multiple precursors are co-isolated in the same window or co-elute chromatographically, thereby deconvoluting chimeric signals and yielding cleaner, more specific MS/MS spectra for confident identification and quantitation.

Deconvolved ZT Scan DIA spectra show significantly less chimeric interference

The value of Q1Dec ZT Scan DIA spectral interpretation is significant. Chimeric spectra complicate the use of orthogonal annotation strategies, such as retention-time alignment. Algorithms that assume a one-to-one correspondence between precursor and product ions can misattribute fragments, leading to incorrect structural hypotheses. In lipidomics and metabolomics contexts—where

structural isomers are prevalent, and differentiation relies on subtle fragmentation signatures—this ambiguity can propagate through annotation pipelines, ultimately reducing the accuracy and reproducibility of reported identifications. However, Q1Dec does not preclude additional deconvolution approaches, such as those performed along the retention-time axis, and multiplexing these approaches is complementary. To illustrate this point, we computed the spectral entropy and normalized spectral entropy for every spectrum in the “NoDec”, “RTDec”, “Q1Dec”, and “RTQ1Dec” sets of PeakID tables exported from the “ZTScan-only” MS-DIAL project and plotted the distribution of entropies for each set of spectra [Figure 4].

The raw entropy distributions [panel a] plot the density of each feature’s spectral entropy from the ZT Scan DIA PeakID spectra obtained from the NoDec, Q1Dec, RTDec, and RTQ1Dec data sets. Panel b shows the density of the normalized spectral entropy, computed using the same features and normalized by the number of peaks in the spectrum, so it ranges from 0 to 1. To classify a feature as clean or noisy, consider spectral entropy, raw entropy, and normalized entropy: a “clean” spectrum is one with minimal noise and is characterized by spectral entropy < 3 for raw entropy and < 0.8 for normalized entropy, as suggested by the software. As shown in both panels, ZT Scan MS/MS data without deconvolution have ~45% of

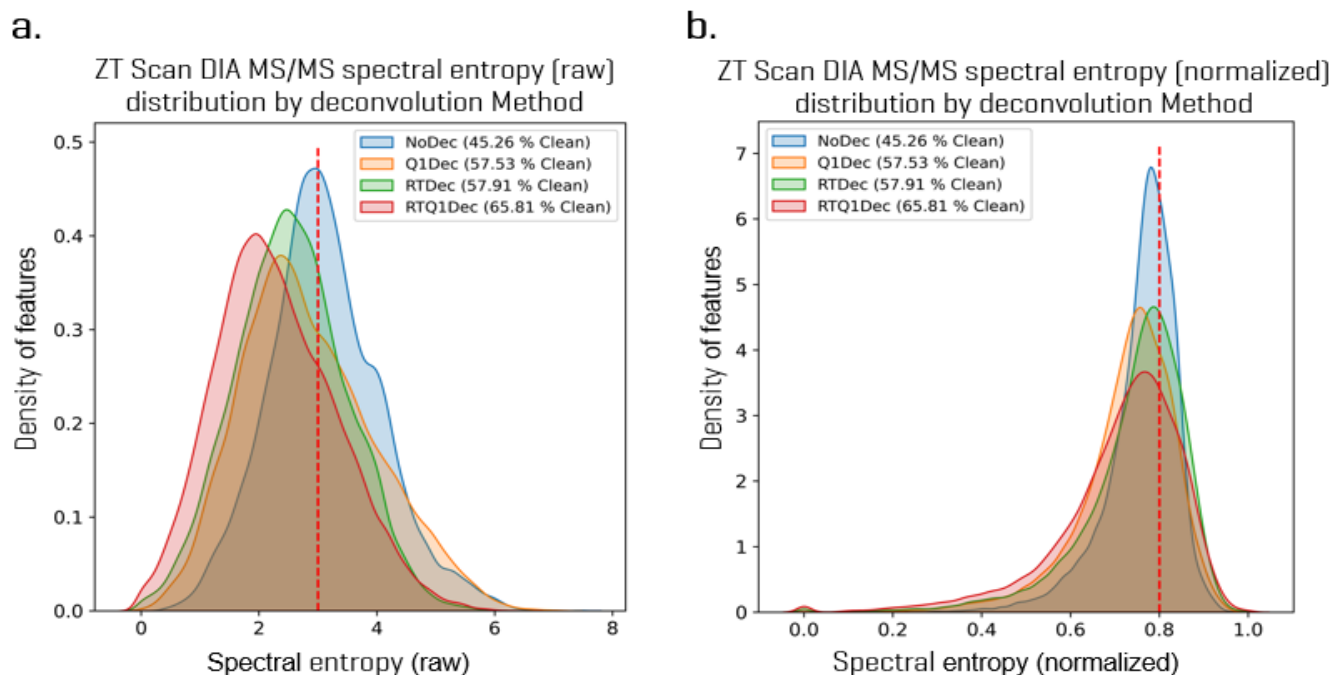


Figure 4. The effects of different types of deconvolution on chimeric interference (spectral entropy). [a] Raw and [b] normalized spectral entropy distributions for ZT Scan DIA PeakID features obtained from “NoDec,” “Q1Dec,” “RTDec,” and “RTQ1Dec” datasets. The overlaid dashed red lines at entropy = 3.0 [panel a] and normalized entropy = 0.8 [panel b] indicate the thresholds used to classify features as “clean” or “noisy.” A feature is considered clean only if it falls to the left of both lines [i.e., satisfies both the raw and normalized entropy criteria simultaneously].

Table 5. Summary of spectral entropy calculations with *in-silico* deconvolution simulation using PeakID results generated by MS-Dial.

Sample ID	% Features with a clean MS/MS spectrum			% Features with deconvolved MS/MS		
	DDA	SWATH	ZT-Scan DIA	DDA	SWATH	ZT-Scan DIA
LbP_1	31.1	52.4	64.2	45.0	40.9	76.1
LbP_2	31.9	54.2	66.2	43.8	40.9	76.8
LbP_3	28.6	49.5	64.2	41.1	40.9	75.4
LbP_4	33.5	56.2	67.4	46.6	42.4	77.7
LiC_3	27.9	52.2	66.6	41.9	40.3	76.0
LiM_3	32.5	54.6	66.3	47.0	42.8	76.8
LiM_4	32.8	55.4	65.6	46.6	40.7	77.3
UI_1	32.5	52.3	64.8	44.6	40.9	76.7
UI_3	32.1	54.4	66.4	44.5	42.6	78.1
UI_4	32.7	55.6	66.1	45.9	42.0	77.0
Average	31.5	53.7	65.8	44.7	41.4	76.8

spectra classified as clean. Q1Dec and RTDec, on their own, increased the percentage of clean spectra to ~58%. The combination of Q1Dec and RTDec increases this percentage to ~66% clean.

To highlight the combined power of comprehensive MS/MS coverage and deconvolution, we summarize and report the results of our entropy calculations and *in silico* deconvolution simulation as a percentage of the total detected features in the sample’s PeakID table from the “All-Modes” project in Table 5. Deconvoluted ZT Scan DIA spectra are cleaner than those derived from DDA (~71% vs. ~32%) and are ~20% cleaner than SWATH data. In aggregate, these results demonstrate the utility of multiplexing deconvolution strategies to improve data quality and, consequently, reference-matching of data to metabolites. Both RTDec and Q1Dec alone improve the percentage of

features with clean MS/MS spectra, but combining the approaches yields the highest percentage of clean spectra.

More IDs with higher confidence by using ZT Scan DIA

Quantifying spectral purity from a theoretical perspective, as demonstrated by spectral entropy calculations, is a useful way to

Table 6. Number and quality of reference-matched metabolites by MS-Dial software for DDA, SWATH, and ZT-Scan DIA metabolomics analysis

Project	Features with a library	Features with a match
	match	score ≥ 1.6
DDA	337	302
SWATH	334	282
ZT-Scan DIA	489	416
All-Modes	489	431

Figure 5. A comparison of DDA vs. ZT Scan DIA spectra for Glu-Asp and the effects of deconvolution. Upper panels show the raw MS/MS spectra for Glu-Asp acquired by DDA (upper left) and ZT Scan DIA (upper right), with the ZT-Scan DIA, even in raw form, displaying a “cleaner” MS/MS spectrum. The lower panels show the effect on the ZT Scan DIA spectrum for Glu-Asp after Q1 deconvolution (lower left) and both Q1 and RT deconvolutions (lower right). The overall complexity of the spectra is reduced through deconvolution.

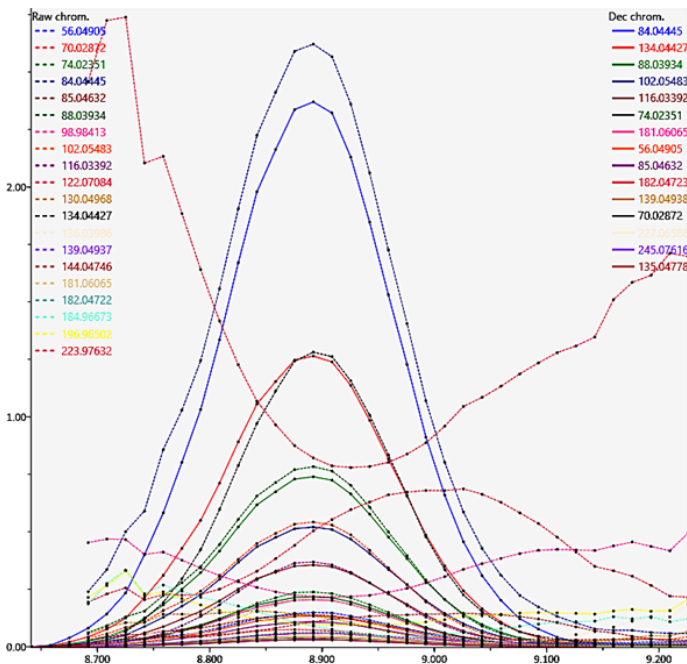
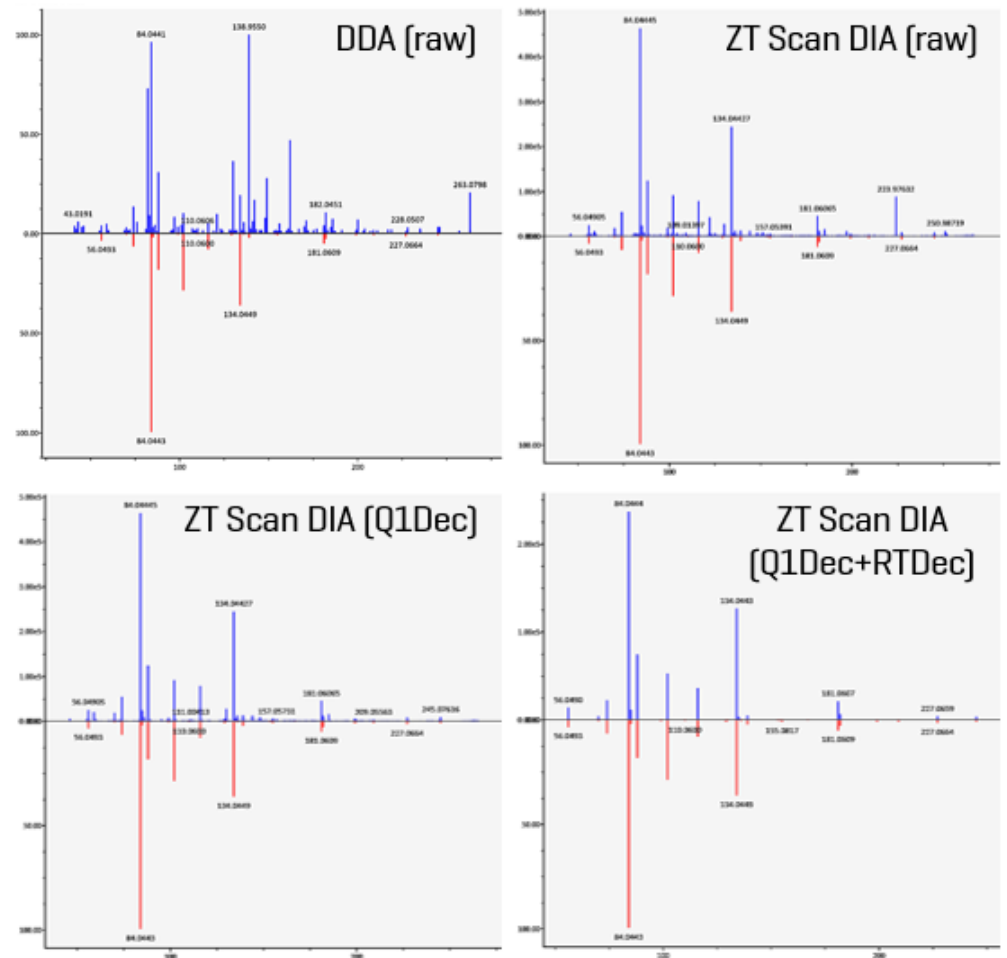


Figure 6. Overlay of XIC of Glu-Asp in raw vs. deconvoluted ZT Scan DIA data acquired on the Zeno TOF 8600 system.

understand how deconvolution affects spectral clarity. However, the impact of deconvolution on improving identification rates and boosting confidence in a metabolomics experiment is paramount. Chimeric spectra are problematic only when they interfere with spectral matching and, ultimately, high-quality identification. In these experiments, the raw MS/MS spectra acquired with ZT Scan DIA are nearly 100% chimeric. However, the results demonstrate that the highest number of library matches is obtained when ZT Scan DIA spectra are deconvoluted using Q1Dec and RTDec. Not only is the number of matches higher, but the quality of the match scores is also higher [Table 6].

To illustrate the MS-DIAL deconvolution process and the resulting spectral decontamination, screen captures are shown in Figures 5 and 6. Figure 5 shows two fundamental observations. First, the upper panels present the spectrum for Glu-Asp acquired by DDA [upper left] and ZT Scan DIA [upper right] for comparison. The purpose of the figure is not to detail the individual fragment masses but rather to present an overall assessment of the complexity of the MS/MS spectra. Interestingly, the DDA MS/MS spectrum is the most complex and exhibits the highest noise, likely due to non-optimal precursor selection for fragmentation. Comparatively, the ZT Scan DIA spectrum, while still chimeric, is less complex. In the lower panels, the effects of MS-DIAL-facilitated Q1 deconvolution [lower left] and multiplexed Q1 and RT deconvolution [lower right] on the spectral complexity are shown. The combination of

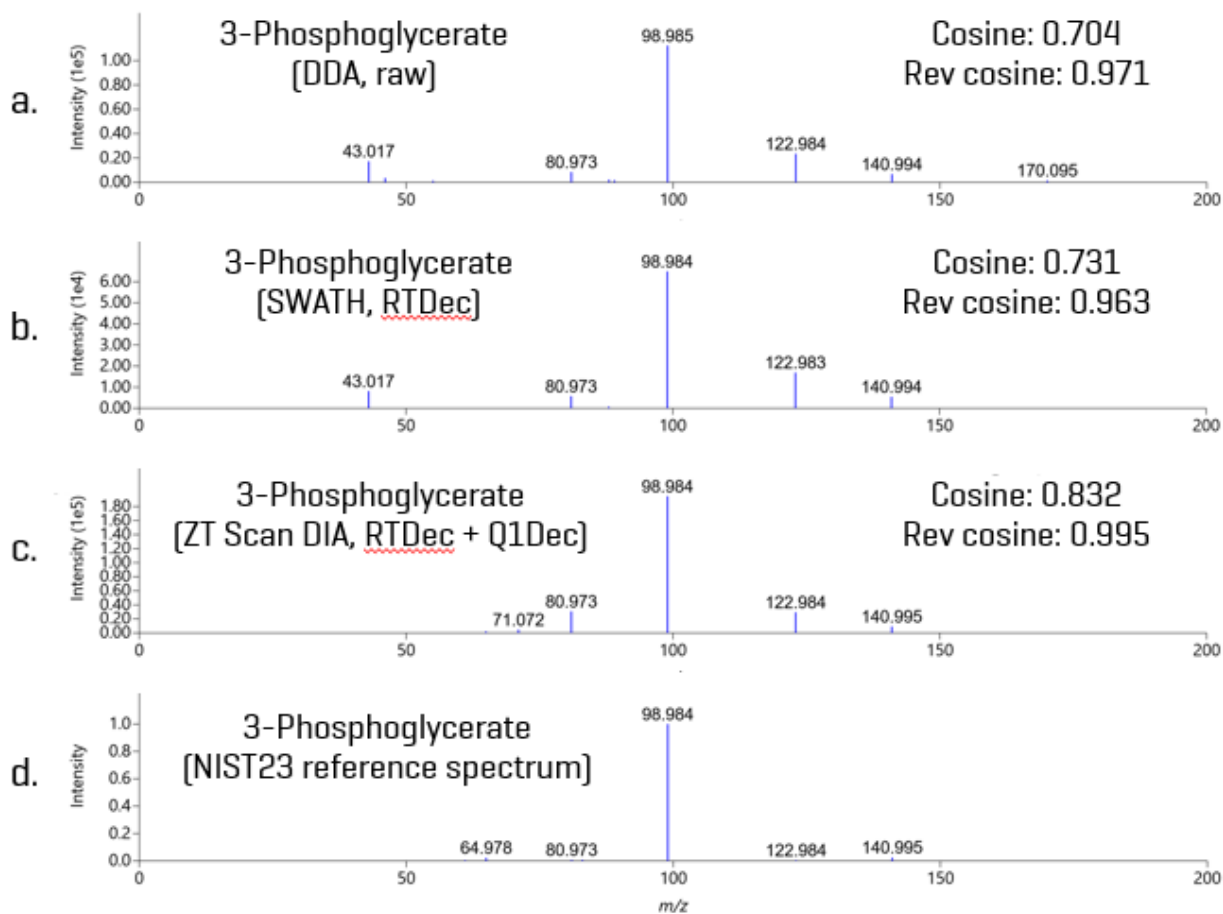


Figure 7. Comparison of MS/MS spectra for 3-phosphoglycerate acquired by DDA [a], SWATH with RTDec [b], and ZT Scan DIA with RTDec + Q1 Dec [c]. Panel D shows the reference spectrum for 3-phosphoglycerate from the NIST23 library. The similarity scores of the acquired vs. reference spectra show that the deconvoluted ZT SCAN DIA spectrum has the highest quality, with a cosine value of 0.832.

Q1Dec and RTDec clearly demonstrates MS-DIAL's ability to "clean" the MS/MS spectrum and enable a high-quality reference match to Glu-Asp. Interestingly, the initial analysis of DDA data using MS-DIAL did not identify Glu-Asp, but because it was the same feature from the same sample, we manually adjusted the library match to ensure consistency.

Figure 6 shows the composite XIC for Glu-Asp, with the legend for the raw XIC on the left and the Q1 and RT deconvoluted data on the right. Although the data are overlaid, it is readily apparent visually which XIC fragments are associated with Glu-Asp at 8.87 min, and which fragments are from matrix interference and/or chimeric fragments.

A final example of how deconvolution of ZT Scan DIA data improves spectral quality compared to other scan modes is shown in Figure 7, which presents the processed 3-phosphoglycerate spectra obtained in DDA, SWATH, and ZT Scan from the same sample and compares them to the reference library spectrum from the NIST23 database. The similarity of the acquired data [panels a-c] was compared to the reference spectrum from the NIST23 library [d]. Cosine similarity [dot product] is a widely applied metric for evaluating the alignment between two vectors, such as spectral profiles or molecular feature embeddings, by measuring the cosine of the angle between them independent of magnitude. Values approaching 1 indicate high similarity, while values

near 0 or negative denote weak or dissimilar relationships. This metric, part of the overall quality score in MS-DIAL, provides a robust means of assessing similarity in high-dimensional analytical datasets.

Conclusions

ZT Scan DIA on the ZenoTOF 8600 system, combined with advanced deconvolution strategies in MS-DIAL, represents a substantive advance for untargeted metabolomics workflows. The data presented here clearly demonstrate that conventional assumptions regarding DDA superiority for spectral quality are no longer valid under modern acquisition and processing paradigms.

Although DDA remains widely used due to its perceived spectral selectivity, this study confirms that a significant proportion of DDA MS/MS spectra (>50%) are inherently chimeric, even when narrow isolation windows and high-Top N methods are employed. This intrinsic limitation reduces identification rates, reduces reproducibility, and limits MS/MS coverage to approximately half of detected features, even at ultra-fast acquisition rates.

In contrast, ZT Scan DIA enables near-complete MS/MS coverage (>99% of features) while leveraging quadrupole-axis deconvolution to

resolve co-isolated precursors at sub-Da resolution, independent of physical isolation width. When combined with retention-time-based deconvolution, this approach delivers a marked improvement in spectral purity, producing approximately twice as many “clean” spectra as DDA and outperforming conventional SWATH DIA workflows.

Critically, these improvements in spectral clarity translate directly into higher identification rates and more confident library matches [Table 6]. ZT Scan DIA datasets processed with combined Q1Dec and RTDec not only yield the highest number of annotations but also exhibit superior spectral similarity scores, underscoring the practical impact of reducing chimeric spectra on downstream metabolite identification.

These findings highlight several key conclusions:

- Chimeric interference is pervasive across all acquisition modes and represents a primary barrier to confident metabolite identification.
- Even with high-coverage [top 85 precursors] DDA experiments at unit resolution, ID rate is reduced due to a large fraction of chimeric spectra that cannot be cleaned.
- Modern, open-source software tools with built-in deconvolution [such as MS-DIAL] facilitate DIA data.
- Dynamic isolation windows schemes outperform narrow, static windows.
- Hardware-enabled innovations such as ZT Scan DIA, when paired with orthogonal deconvolution strategies, effectively address the challenge of chimeric interference.
- Comprehensive MS/MS coverage combined with post-acquisition deconvolution is more advantageous than selective acquisition alone.

Overall, ZT Scan DIA establishes a new performance benchmark for DIA-based metabolomics by unifying high coverage, improved spectral purity, and enhanced identification confidence. This workflow provides a scalable and robust solution for complex biological studies, enabling deeper and more reliable interrogation of the metabolome.

References

- [1] Zeno trap: Defining new levels of sensitivity. [2021] SCIEX white paper, RUO-MKT-19-13373-B. <https://sciex.com/content/dam/SCIEX/pdf/brochures/zeno-trap-whitepaper.pdf>
- [2] Sayers, R, Tran, K, and Walsh, N. Continuing the data independent acquisition [r]evolution: Introducing ZT Scan DIA for quantitative proteomics. SCIEX white paper MKT-31731-A. <https://sciex.com/content/dam/SCIEX/pdf/tech-notes/technology/ztscan-dia-introduction.pdf>
- [3] PRS, Proos, R, Ozbalci, C, Hecht, M, Chiapparino, A, Rupasinga, T, Sayers, R, and Causon, J. [2026] Untargeted, quantitative metabolomics analysis on the ZenoTOF 8600 system using the novel ZT Scan DIA 2.0 workflow. SCIEX white paper MKT-37675-B. <https://sciex.com/tech-notes/life-science-research/metabolomics/untargeted-quantitative-metabolomics-analysis-on-zenotof8600>
- [4] Stein, S. E. An Integrated Method for Spectrum Extraction and Compound Identification from Gas Chromatography/Mass Spectrometry Data. *J. Am. Soc. Mass Spectrom.* 1999, 10 [8], 770–781. [https://doi.org/10.1016/S1044-0305\(99\)00047-1](https://doi.org/10.1016/S1044-0305(99)00047-1)
- [5] Tsugawa, H.; Cajka, T.; Kind, T.; Ma, Y.; Higgins, B.; Ikeda, K.; Kanazawa, M.; Vandergheynst, J.; Fiehn, O.; Arita, M. MS-DIAL: Data-Independent MS/MS Deconvolution for Comprehensive Metabolome Analysis. *Nature Methods* 2015 12:6 2015, 12 [6], 523–526. <https://doi.org/10.1038/nmeth.3393>
- [6] Yin, Y.; Wang, R.; Cai, Y.; Wang, Z.; Zhu, Z. J. DecoMetDIA: Deconvolution of Multiplexed MS/MS Spectra for Metabolite Identification in SWATH-MS-Based Untargeted Metabolomics. *Anal. Chem.* 2019, 91 [18], 11897–11904. <https://doi.org/10.1021/ACS.ANALCHEM.9B02655>
- [7] Tada, I.; Chaleckis, R.; Tsugawa, H.; Meister, I.; Zhang, P.; Lazarinis, N.; Dahlén, B.; Wheelock, C. E.; Arita, M. Correlation-Based Deconvolution [CorrDec] To Generate High-Quality MS² Spectra from Data-Independent Acquisition in Multisample Studies. *Anal. Chem.* 2020, 92 [16], 11310–11317. <https://doi.org/10.1021/ACS.ANALCHEM.0C01980>
- [8] Stancliffe, E.; Schwaiger-Haber, M.; Sindelar, M.; Patti, G. J. DecoID Improves Identification Rates in Metabolomics through Database-Assisted MS/MS Deconvolution. *Nature Methods* 2021 18:7 2021, 18 [7], 779–787. <https://doi.org/10.1038/s41592-021-01195-3>
- [9] Stancliffe, E.; Gandhi, M.; Guzior, D. V.; Mehta, A.; Acharya, S.; Richardson, A.; Cho, K.; Cohen, T.; Patti, G. J. MassID Provides near Complete Annotation of Metabolomics Data with Identification Probabilities. *bioRxiv* 2026, 2026.02.11.704864. <https://doi.org/10.64898/2026.02.11.704864>
- [10] Röst, H. L.; Rosenberger, G.; Navarro, P.; Gillet, L.; Miladinoviá, S. M.; Schubert, O. T.; Wolski, W.; Collins, B. C.; Malmström, J.; Malmström, L.; Aebersold, R. OpenSWATH Enables Automated, Targeted Analysis of Data-Independent

- Acquisition MS Data. *Nature Biotechnology* 2014 32:3 2014, 32 [3], 219–223. <https://doi.org/10.1038/nbt.2841>
- [11] Peckner, R.; Myers, S. A.; Jacome, A. S. V.; Egertson, J. D.; Abelin, J. G.; MacCoss, M. J.; Carr, S. A.; Jaffe, J. D. Specter: Linear Deconvolution for Targeted Analysis of Data-Independent Acquisition Mass Spectrometry Proteomics. *Nature Methods* 2018 15:5 2018, 15 [5], 371–378. <https://doi.org/10.1038/nmeth.4643>
- [12] Li, H.; Cai, Y.; Guo, Y.; Chen, F.; Zhu, Z. J. MetDIA: Targeted Metabolite Extraction of Multiplexed MS/MS Spectra Generated by Data-Independent Acquisition. *Anal. Chem.* 2016, 88 [17], 8757–8764. <https://doi.org/10.1021/ACS.ANALCHEM.6B02122>
- [13] Nikolskiy, I.; Mahieu, N. G.; Chen, Y. J.; Tautenhahn, R.; Patti, G. J. An Untargeted Metabolomic Workflow to Improve Structural Characterization of Metabolites. *Anal. Chem.* 2013, 85 [16], 7713–7719. <https://doi.org/10.1021/ac400751j>
- [14] Matsuzawa, Y.; Tokiyoshi, K.; Buyantogtokh, B.; Oka, T.; Causon, J.; Yamamoto, R.; Takeuchi, M.; Takeda, U.; Takahashi, M.; Hasegawa, M.; Ivosev, G.; Cox, D.; Baker, P. R.; Chelur, A.; Bloomfield, N.; Miyamoto, J.; Harayama, T.; Deng, L.; Tsugawa, H. Retrospective Metabolomics via Dual-Dimensional Deconvolution Using ZT Scan DIA 2.0. *bioRxiv* 2025, 2025.08.20.671307. <https://doi.org/10.1101/2025.08.20.671307>
- [15] Messner, C. B.; Demichev, V.; Bloomfield, N.; Yu, J. S. L.; White, M.; Kreidl, M.; Egger, A. S.; Freiwald, A.; Ivosev, G.; Wasim, F.; Zelezniak, A.; Jürgens, L.; Suttorp, N.; Sander, L. E.; Kurth, F.; Lilley, K. S.; Mülleder, M.; Tate, S.; Ralser, M. Ultra-Fast Proteomics with Scanning SWATH. *Nat. Biotechnol.* 2021, 39 [7], 846–854. <https://doi.org/10.1038/S41587-021-00860-4;SUBJMETA=45,475,61,631;KWRD=PROTEOMICS>
- [16] Kim, S.; Thiessen, P. A.; Bolton, E. E. Programmatic Retrieval of Small Molecule Information from PubChem Using PUG-REST. *Methods in Pharmacology and Toxicology* 2018, 1–24. https://doi.org/10.1007/7653_2018_30
- [17] Kim, S.; Thiessen, P. A.; Bolton, E. E.; Bryant, S. H. PUG-SOAP and PUG-REST: Web Services for Programmatic Access to Chemical Information in PubChem. *Nucleic Acids Res.* 2015, 43 [W1], W605–W611. <https://doi.org/10.1093/nar/gkv396>
- [18] Li, Y.; Kind, T.; Folz, J.; Vaniya, A.; Mehta, S. S.; Fiehn, O. Spectral Entropy Outperforms MS/MS Dot Product Similarity for Small-Molecule Compound Identification. *Nature Methods* 2021 18:12 2021, 18 [12], 1524–1531. <https://doi.org/10.1038/s41592-021-01331-z>
- [19] Spectral Entropy and Normalized Entropy in MoNA. MoNA - Mass Bank of North America. <https://mona.fiehnlab.ucdavis.edu/documentation/entropy>

The SCIEX clinical diagnostic portfolio is For In Vitro Diagnostic Use. Rx Only. Product[s] not available in all countries. For information on availability, please contact your local sales representative or refer to <https://sciex.com/diagnostics>. All other products are For Research Use Only. Not for use in Diagnostic Procedures.

Trademarks and/or registered trademarks mentioned herein, including associated logos, are the property of AB Sciex Pte. Ltd. or their respective owners in the United States and/or certain other countries [see www.sciex.com/trademarks].

© 2026 DH Tech. Dev. Pte. Ltd. MKT-38463-A



Headquarters
250 Forest Street, Marlborough,
MA 01752 USA
 Phone 508-383-7700
sciex.com

International Sales
 For our office locations please call the
 division
 headquarters or refer to our website at
sciex.com/offices